

International Journal of Modern Physics: Conference Series
 © World Scientific Publishing Company

RECENT RESULTS FROM LATTICE QCD

CHUAN LIU

*School of Physics and Center for High Energy Physics
 Peking University, Beijing 100871, China
 liuchuan@pku.edu.cn*

Received Day Month Year
 Revised Day Month Year

Recent Lattice QCD results are reviewed with an emphasis on spectroscopic results concerning the charm quark. It is demonstrated that, with accurate computations from lattice QCD in recent years that can be compared with the existing or upcoming experiments, stringent test of the Standard Model can be performed which will greatly sharpen our knowledge on the strong interaction.

Keywords: lattice QCD, charm quark, comparison with experiments.

PACS numbers:12.38.Gc, 11.15.Ha

1. Introduction

In the past ten years or so, considerable progress has been achieved in lattice Chromodynamics (lattice QCD). Here, I will try to review briefly some selected results, with an emphasis on those related to the charm quark, and compare them with the experiments so far or possibly in the near future. For general recent lattice results, please consult the Lattice 2013 website¹ where the talks are available online.

Lattice QCD is a non-perturbative theoretical method that relies on Monte Carlo estimation of physical quantities using gauge field samples that are generated according to a lattice action. Given a lattice action $S = S_g[U_\mu] + S_f[\bar{\psi}, \psi, U_\mu] = S_g[U_\mu] + \bar{\psi}_x \mathcal{M}_{xy}[U_\mu] \psi_y$, where $\mathcal{M}[U_\mu]$ is called the fermion matrix^a, a physical quantity of interest, $\mathcal{O}[\bar{\psi}, \psi, U_\mu]$, which is built from the basic fields is given by the *ensemble average*:

$$\langle \mathcal{O} \rangle = \frac{1}{\mathcal{Z}} \int \mathcal{D}\bar{\psi} \mathcal{D}\psi \mathcal{D}U_\mu \mathcal{O}[\bar{\psi}, \psi, U_\mu] e^{-S[\bar{\psi}, \psi, U_\mu]}. \quad (1)$$

Here the partition function \mathcal{Z} is given by the relevant path integral

$$\mathcal{Z} = \int \mathcal{D}\bar{\psi} \mathcal{D}\psi \mathcal{D}U_\mu e^{-S[\bar{\psi}, \psi, U_\mu]} = \int \mathcal{D}U_\mu e^{-S_g[U_\mu]} \det \mathcal{M}[U_\mu]. \quad (2)$$

^aThe explicit form of $\mathcal{M}[U_\mu]$ depends on the type of lattice fermion (staggered, Wilson, etc.) used.

2 *C. Liu*

Following the above equations, a typical lattice calculation therefore consists of two steps: In the first step, also known as the generation step, one generates the gauge field configurations according to the probability distribution: $P[U_\mu] = \mathcal{Z}^{-1} e^{-S_g[U_\mu]} \det \mathcal{M}[U_\mu]$ and stores them for later usage; In the second step, also known as the measurement step, any interested observable $\mathcal{O}[\bar{\psi}, \psi, U_\mu]$ is measured from the pre-stored gauge field configurations with the quark and anti-quark fields in the corresponding observable replaced by the corresponding quark propagators, which are relevant matrix elements of $\mathcal{M}^{-1}[U_\mu]$, in a particular gauge field background. Note that the fermion matrix $\mathcal{M}[U_\mu]$ is diagonal in flavor space. Therefore, the determinant of the matrix in Eq. (2) is in fact a product of determinants for each quark flavor. Depending on how many flavors are kept in the generation step, we call them N_f flavor lattice QCD.^b

2. Spectrum calculations

2.1. Hadron Masses, conventional computation

To compute the mass values of hadrons, one starts from a set of interpolating operators $\{\mathcal{O}_\alpha(t) : \alpha = 1, 2, \dots, N\}$.² These operators carry the correct quantum numbers such that the state $\mathcal{O}_\alpha^\dagger(t)|\Omega\rangle$, with $|\Omega\rangle$ being the QCD vacuum state, has the same quantum numbers as those of the hadron in question. In lattice Monte Carlo simulations, the following correlation matrix is measured:

$$\mathcal{C}_{\alpha\beta}(t) = \langle \Omega | \mathcal{O}_\alpha(t) \mathcal{O}_\beta^\dagger(0) | \Omega \rangle . \quad (3)$$

On the other hand, it is known that the same correlation matrix is given by

$$\mathcal{C}_{\alpha\beta}(t) = \sum_n \frac{e^{-E_n t}}{2E_n} Z_\alpha^{(n)} Z_\beta^{(n)*} , \quad (4)$$

where the summation is over all eigenstates (labelled by n) of the Hamiltonian with the E_n 's being the corresponding eigenvalues. The measured correlation matrix $\mathcal{C}_{\alpha\beta}(t)$ is then passed through a standard variational calculation, also known as the generalized eigenvalue problem (GEVP),^{3,4} for some given t_0 :

$$\mathcal{C}_{\alpha\beta}(t) v_\beta^{(n)} = \lambda^{(n)}(t) \mathcal{C}_{\alpha\beta}(t_0) v_\beta^{(n)} . \quad (5)$$

Here $\lambda^{(n)}(t)$'s yield the eigenvalues of the Hamiltonian, namely the E_n 's via

$$\lambda^{(n)}(t) \sim e^{-E_n(t-t_0)} \left[1 + O\left(e^{-\Delta E(t-t_0)}\right) \right] , \quad (6)$$

while the eigenvectors $v_\beta^{(n)}$ are related to the corresponding overlap $Z_\alpha^{(n)}$.⁴

Standard light hadron spectroscopy has been studied by various groups in recent years, see e.g. Ref. 5. Hadrons containing the heavy quarks have also been studied. In Fig. 1, we have shown the heavy meson spectrum from HPQCD collaboration

^bQuenched lattice QCD corresponds to $N_f = 0$ in this sense.

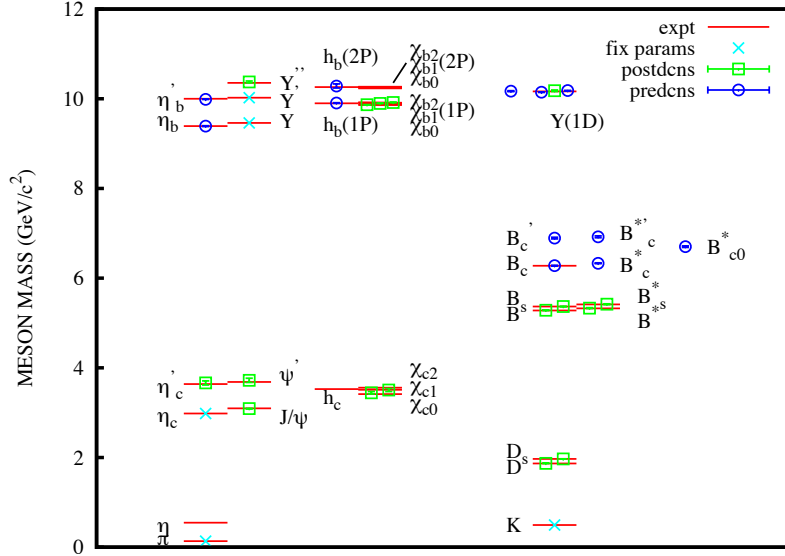


Fig. 1. Heavy meson spectrum obtained from $N_f = 2 + 1 + 1$ lattice QCD, taken from the paper by HPQCD collaboration.⁶

obtained using $N_f = 2 + 1 + 1$ staggered quark configurations.⁶ It is seen that, both post-dictions and predictions agree with the experiments, where available, astonishingly well.

2.2. Hadron Masses, multi-hadron scattering effects

However, one should keep in mind that, in principle, these E_n 's are *not* the mass values of the hadrons. The eigenvalue of the QCD Hamiltonian in a particular symmetry sector is only approximately equal to the mass of the hadron if the hadron being studied is a narrow resonance within strong interaction.^c Therefore, to really study a genuine hadronic resonance, one should study the scattering of hadrons. In fact, Lüscher has established a formalism⁷ in which the eigenvalues of the finite-volume Hamiltonian are related to the scattering phases of the two particles.⁸

In the simplest case (single channel, s-wave scattering, neglecting higher l contributions, etc.), this relation reads:

$$\tan \delta_0(E) = \frac{\pi^{3/2} q}{\mathcal{Z}_{00}(1, q^2)} \quad , \quad (7)$$

where $\mathcal{Z}_{00}(1, q^2)$ is the zeta function that can be computed accurately and q is

^cIf the hadron is stable in QCD, then the E_n is *indeed* the mass of the hadron. But for resonances, which is true for majority of the hadrons, this is not the case.

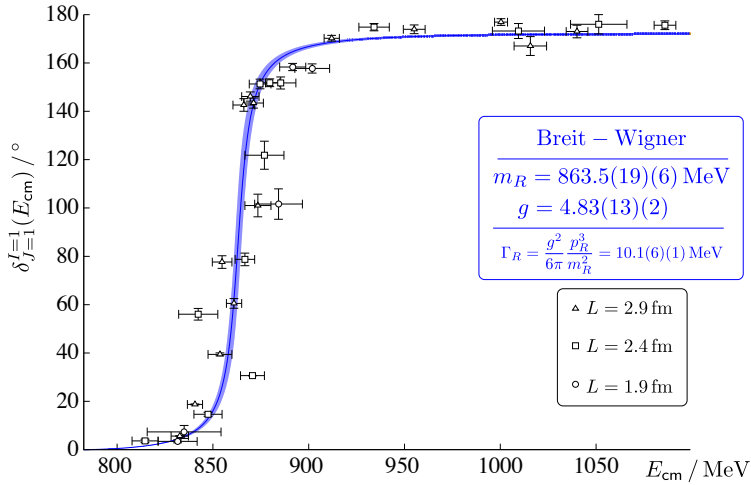
4 *C. Liu*


Fig. 2. Phase shifts of $\pi\pi$ scattering in the $I = J = 1$ channel calculated from lattice QCD using Lüscher’s formalism, taken from a paper by the Hadron Spectrum Collaboration.⁹

related to E via

$$E = \sqrt{m_1^2 + \bar{k}^2} + \sqrt{m_2^2 + \bar{k}^2}, \quad q \equiv \frac{\bar{k}L}{2\pi}. \quad (8)$$

The lattice calculation goes the same way as we described above with the exception that the interpolation operators being used, namely the operators $\{\mathcal{O}_\alpha(t) : \alpha = 1, 2, \dots, N\}$, should also include the two-particle operators. Using Lüscher’s formalism, one simply obtains the energy eigenvalues E_n ’s which are then substituted into Lüscher formula for $\delta_0(E_n)$. For small momentum close to the threshold, one could use the effective range expansion

$$k \cot \delta(E) = \frac{1}{a_0} + \frac{1}{2}r_0 k^2 + \dots \quad (9)$$

with a_0 being the scattering length and r_0 the effective range.

Lüscher’s formula has been generalized to various cases, see e.g. Ref. 10 and references therein. It has also been utilized successfully in lattice studies of hadronic resonances in recent years, see e.g. Ref. 2, 8 and references therein. A very good example is the lattice QCD study of the ρ meson, a typical hadronic resonance in the $I = J = 1$ channel of $\pi\pi$ scattering. In Fig 2, taken from Ref. 9, we have shown the phase shifts of $\pi\pi$ scattering in the $I = 1, J = 1$ channel computed within Lüscher’s formalism.

2.3. Scattering of Charmed mesons

Recently, there have been numerous new hadronic structures observed which contain charm and anti-charm quark. These have been termed the XYZ particles, see

Refs 11, 12, 13. What is noticeable is that many of these newly observed states are close to the threshold of two known charmed mesons. For example, the $X(3872)$ is close to the threshold of D and D^* and so is the newly discovered $Z_c^\pm(3900)$.¹⁴

Several years ago, CLQCD has studied the $Z(4430)$ state observed by BELLE collaboration in quenched lattice QCD using Lüscher formalism.¹⁵ Asymmetric volumes were used to investigate the low-momentum behavior of the scattering phase close to the threshold of D^* and a \bar{D}_1 . The investigation was done in the channel of $J^P = 0^-$ and the interaction between the D^* and a \bar{D}_1 was found to be attractive but not strong enough to form a genuine bound state.

Recently, Prelovsek *et al* have studied the case of $X(3872)$ using $N_f = 2$ improved Wilson fermion configurations.¹⁶ They claim that they have found some evidence for the state. With the same set of configurations, they have also studied the case of $Z_c(3900)$ with no signal of the state.¹⁷

In summary, the study for these XYZ states are still an on-going project. Lattice results obtained so far are still not systematic (most of them are at one lattice spacing, one volume, one pion mass etc.) and therefore one still cannot draw definite conclusions yet. The situation is still somewhat murky and more work needs to be done in the future to clarify the nature of these states from lattice QCD.

2.4. Decay constants and the story of f_{D_s}

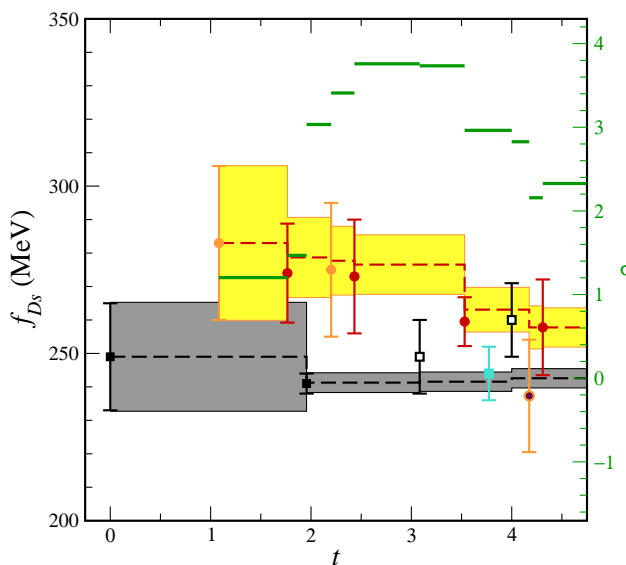


Fig. 3. The history of f_{D_s} till the end of 2009, taken from A. Kronfeld's review talk "The f_{D_s} puzzle" for PIC2009.

6 *C. Liu*

For a pseudoscalar meson, the decay constant is defined via the matrix elements

$$\begin{cases} \langle \Omega | \bar{s} \gamma_\mu \gamma_5 c | D_s(p) \rangle = i f_{D_s} p_\mu, \\ (m_c + m_s) \langle \Omega | \bar{s} \gamma_5 c | D_s(p) \rangle = -m_{D_s}^2 f_{D_s} \end{cases} \quad (10)$$

with the two definitions related to each other by PCAC.

This quantity can be computed accurately in lattice QCD which then can be compared with the experiments. Around the year of 2008, some puzzling effects occurred that created a 3.8σ difference in the comparison of the lattice results and the experiments. For a more detailed description about this dilemma, the reader is referred to A. Kronfeld’s review talk “The f_{D_s} puzzle” in the proceedings of Physics In Collisions in 2009 (PIC2009).¹⁸

Basically, the puzzle came about because around 2008, the error of the lattice computation dropped significantly due to the HPQCD’s new result on f_{D_s} .¹⁹ The tension with the experiments then increased to about 3.8σ around that time, making people contemplating about possible new physics to clarify the puzzle. However, as time goes on, this tension is finally eased, mainly due to the fact that new experimental results²⁰ came down quite a bit while the lattice result also moves up a little, so that by the end of 2010, the discrepancy is only 1.6σ .²¹ Most recent lattice calculations yields compatible results with those in 2009, with the errors further reduced, see e.g. C. Bernard’s talk at Lattice 2013.²² Note that, although there is no significant “puzzle” right now for f_{D_s} , the story of the the so-called “ f_{D_s} puzzle” has given us a very instructive lesson: precise comparison between the experiments and theory is vital in this game. In the future, should there be more accurate experimental results come about, e.g. at BESIII, there could be further puzzles and by resolving these puzzles, we could sharpen our knowledge about QCD and beyond.

3. Radiative transitions and decays of charmonia

Charmonium states play an important role in our understanding of QCD. For charmonia lying below the open charm threshold, radiative decays are important to illuminate the structure of these states. Recently and in the years to come, more experimental data are being accumulated at BEPCII which will enable us to make precise comparison between the experiments and theory.

To lowest order in QED, the amplitude for $J/\psi \rightarrow \gamma H$ is given by

$$M_{r,r_\gamma,r_H} = \epsilon_\mu^*(\vec{q}, r_\gamma) \langle H(\vec{p}_f, r_H) | j^\mu(0) | J/\psi(\vec{p}_i, r) \rangle, \quad (11)$$

where \vec{p}_i/\vec{p}_f is the initial/final three-momentum of the hadron, respectively, while $\vec{q} = \vec{p}_i - \vec{p}_f$ is the three-momentum of the real photon. We use r, r_H, r_γ to denote the polarizations of the relevant particles. ^d $\epsilon_\mu(\vec{q}, r_\gamma)$ is the polarization

^dIf the final hadron H is a scalar, then the label r_H is not needed.

four-vector of the real photon and $j_{e.m.}^\mu(0)$ stands for the electromagnetic current operator due to the quarks. We emphasize that the hadronic matrix element $\langle H(\vec{p}_f, r_H) | j^\mu(0) | J/\psi(\vec{p}_i, r) \rangle$ is non-perturbative in nature and consequently should be computed using non-perturbative methods like lattice QCD.

It turns out that the above mentioned matrix element can be obtained from the following three-point correlation function,

$$\Gamma_{i,\mu,j}^{(3)}(\vec{p}_f, \vec{q}; t_f, t) = \frac{1}{T} \sum_{\vec{y}, \tau=0}^{T-1} e^{-i\vec{q}\cdot\vec{y}} \langle \Phi^{(i)}(\vec{p}_f, t_f + \tau) J_\mu(\vec{y}, t + \tau) O_{V,j}(\vec{0}, \tau) \rangle, \quad (12)$$

where $J_\mu = \bar{c}\gamma_\mu c$ is the vector current of the charm quark. By measuring three-point function in Eq. (12) together with relevant two-point functions, one could obtain the desired hadronic matrix element $\langle H(\vec{p}_f, r_H) | j^\mu(0) | J/\psi(\vec{p}_i, r) \rangle$.

For charmonium states various lattice computations, both quenched²³ and unquenched,^{24, 25, 26} have been performed and the results can be compared with the corresponding experiments. For example, for the radiative transition rate $J/\psi \rightarrow \gamma\eta_c$, it is parameterized by a form factor $V(q^2)$:

$$\langle \eta_c(p') | \bar{c}\gamma^\mu c | J/\psi(p) \rangle = \frac{2V(q^2)}{M_{J/\psi} + M_{\eta_c}} \epsilon^{\mu\alpha\beta\gamma} p'_\alpha p_\beta \epsilon(p)_\gamma, \quad (13)$$

and the decay rate is given by the value of $V(0)$. The HPQCD result finally gives:²⁵

$$V(0) = 1.90(7)(1), \quad (14)$$

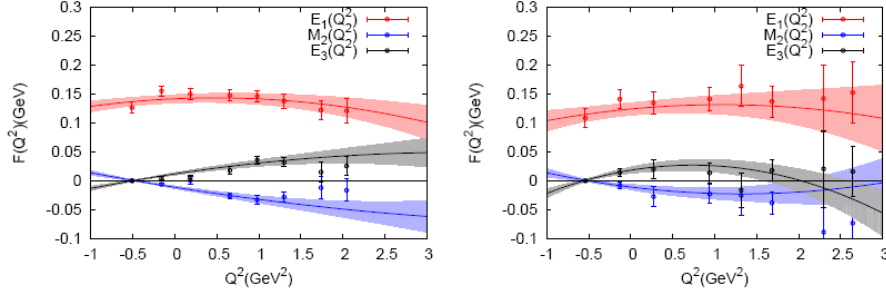
which is larger than the experimental value from CLEO²⁷ by about 1.7σ . Another lattice calculation using 2 flavors of twisted mass fermions yields even larger (but compatible with that of HPQCD) result.²⁶ Right now, the experimental error is larger than those in lattice computations. Later on, more accurate experiments at BESIII will surely bring more stringent test to this comparison.

Not only can one computes transitions among charmonium states, one could also compute the radiative transitions of J/ψ to pure-gauge glueballs on the lattice. This has been done recently by CLQCD in quenched lattice QCD.^{28, 29} The relevant hadronic matrix element $\langle G(\vec{p}_f, r_G) | J_\mu(0) | V(\vec{p}_i, r) \rangle$ are expanded in terms of form factors and known kinematic functions, see e.g. Ref. 30. Take the tensor glueball as an example, we have

$$\begin{aligned} \langle G(\vec{p}_f, r_G) | J_\mu(0) | V(\vec{p}_i, r) \rangle &= \alpha_1^\mu E_1(Q^2) + \alpha_2^\mu M_2(Q^2) \\ &+ \alpha_3^\mu E_3(Q^2) + \alpha_4^\mu C_1(Q^2) + \alpha_5^\mu C_2(Q^2), \end{aligned} \quad (15)$$

where α_i^μ 's are kinematic functions and E_1, M_1, E_2 etc. are the form factors. For the scalar glueball, one only needs two form factors $E_1(Q^2)$ and $C_1(Q^2)$ instead.

The physical decay rates for $J/\psi \rightarrow \gamma G$ only depend on the values of the form

8 *C. Liu*

 Fig. 4. The extracted form factors for tensor glueball at two different lattice spacings.²⁹

 factors at $Q^2 = 0$:

$$\Gamma(J/\psi \rightarrow \gamma G_{0^{++}}) = \frac{4\alpha|\vec{p}_\gamma|}{27M_{J/\psi}^2} |E_1(0)|^2, \quad (16)$$

$$\Gamma(J/\psi \rightarrow \gamma G_{2^{++}}) = \frac{4\alpha|\vec{p}_\gamma|}{27M_{J/\psi}^2} (|E_1(0)|^2 + |M_2(0)|^2 + |E_3(0)|^3). \quad (17)$$

Therefore, the computed matrix elements at various values of Q^2 are then fitted using a polynomial in Q^2 to extract the relevant values at $Q^2 = 0$. In Fig. 4, we show the case for the tensor glueball at two different lattice spacings. After the continuum extrapolation, the physical values for these form factors are obtained which then gives us the prediction of relevant decay rates.

Needless to say, the so-called pure-gauge glueballs are not physical objects that can be measured directly in experiments. In real world they mix with ordinary hadrons with the same quantum numbers. However, the above mentioned lattice calculation can provide us with important information about the pure-gauge glueball component in the measured hadronic states. For example, this calculation helps to clarify, say in the scalar channel, which of the three candidates $f_0(1370)$, $f_0(1500)$ and $f_0(1710)$ contains more glueball component and can thus be regarded as the best candidate for the scalar glueball.²⁸

4. The anomalous magnetic moment of the muon

A precisely measured quantity that brings significant deviation from the prediction of the Standard Model (SM) is the anomalous magnetic moment of the muon. The definition of this quantity is

$$a_\mu = (g_\mu - 2)/2. \quad (18)$$

This is one of the most accurately measured quantities:

$$a_\mu^{\text{exp}} = 11659208.9(5.4)(3.3) \times 10^{-10}. \quad (19)$$

The same quantity predicted by the Standard Model is, however,

$$a_\mu^{\text{SM}} = 11659180.2(0.2)(4.2)(2.6) \times 10^{-10}. \quad (20)$$

The difference of the above two equations is

$$\Delta a_\mu \equiv a_\mu^{\text{exp}} - a_\mu^{\text{SM}} = 287(63)(49) \times 10^{-11}. \quad (21)$$

This is roughly a 3.6σ effect, one of the remaining “puzzles” in SM.

Although the major part of a_μ comes from QED, the major *theoretical uncertainty* comes from the hadronic contributions, denoted as a_μ^{Had} , and is given by

$$a_\mu^{\text{Had}} = a_\mu^{\text{HVP}} + a_\mu^{\text{HLbL}} + \dots \quad (22)$$

Here, the leading contribution comes from Hadronic Vacuum Polarisation (HVP), a_μ^{HVP} , that can be measured experimentally with the help of dispersion relations. The next-order correction, the Hadronic Light-by-light scattering (HLbL), a_μ^{HLbL} , cannot be related to experimentally measurable quantities and currently relies on modelling, see e.g. PDG reviews.³¹

There have been several lattice attempts to compute a_μ^{HVP} since past decade,^{32,33,34,35,36,37} which can be related to the current-current correlator in QCD:

$$a_\mu^{\text{HVP}} = \alpha^2 \int_0^\infty \frac{dQ^2}{Q^2} w(Q^2/m_\mu^2) \hat{\Pi}(Q^2), \quad (23)$$

where $w(Q^2/m_\mu^2)$ is a known function;³² The quantity $\hat{\Pi}(Q^2) = \Pi(Q^2) - \Pi(0)$ is defined via:

$$\begin{cases} \Pi_{\mu\nu}(Q) \equiv (Q_\mu Q_\nu - Q^2 \delta_{\mu\nu}) \Pi(Q^2) \\ \Pi_{\mu\nu}(Q) = \int d^4x e^{iQ \cdot x} \langle \Omega | T [J_\mu(x) J_\nu(0)] | \Omega \rangle \end{cases} \quad (24)$$

In principle, the current-current correlator $\langle \Omega | T [J_\mu(x) J_\nu(0)] | \Omega \rangle$ can be computed using standard methods in lattice QCD. However, it does pose several challenges for the current state of the art lattice computations. It turns out that this quantity is dominated by contributions at low Q^2 , typically $Q^2 \sim 1\text{GeV}^2$, which is difficult for current realistic lattice calculations. It also requires rather delicate error controlling in lattice extrapolations in order to match the precision of the experimental measurements. Right now, the lattice results are in no comparison with those using dispersion relations yet, as far as the errors are concerned. However, with more and more lattice groups are joining the game, see e.g. Lattice 2013 talks,³⁸ hopefully we will get a better control in the years to come.

In Fig. 5, I show a summary figure taken partly from Gregory’s talk³⁹ at Lattice 2013. I have added another new point from ETMC collaboration using $2 + 1 + 1$ twisted mass fermion configurations.⁴⁰ All available lattice data for $a_\mu^{\text{HVP}} \equiv a_\mu^{\text{had,LO}}$ are summarized together with those obtained using dispersion relations. It is seen that, although some of the lattice results are compatible with those of dispersive analysis, they still need much improvement to reduce the errors in order to match the accuracy for the dispersive analysis which is comparable to that of the experimental ones.

10 *C. Liu*

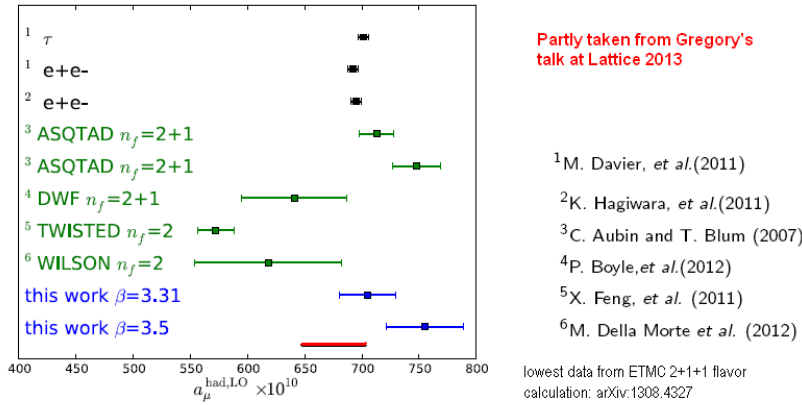


Fig. 5. The current status of lattice computation for a_μ , taken partly from Gregory's talk at Lattice 2013.³⁹

5. Conclusions and outlook

In recent years, as a theoretical tool from first principles, lattice QCD has become an important player in relevant field of physics involving the strong interaction. Due to the crossover from quenched to unquenched calculations, more and more lattice results are available that are both practical and accurate enough to be compared with the existing or upcoming experiments. Some of these lattice results are reviewed here in this talk, with an emphasis on the properties involving the charm quark. I have also try to emphasize the interplay between the experimental results and those obtained from lattice computations.

For the hadron masses and decays, we have seen both post-dictions and predictions that agree rather well with the experiments. Lattice computations nowadays can also handle hadron-hadron scattering processes, which not only helps to obtain important information about hadronic interactions for the resonances, but also to clarify some of the newly discovered exotic hadronic states, the so-called XYZ particles. For the radiative transition and decays of charmonium, lattice computations have matured to a stage that a detailed comparison with experiments is possible. It is also possible to offer us information about glueballs in the radiative decays.

Many of the quantities mentioned above can be obtained rather precisely in lattice calculations, thus providing a precision test for QCD. It is important and instructive to compare the available lattice QCD results with the experiments. Some of the lattice results agree with the experiment perfectly: the hyperfine splitting of the charmonium $M_{J/\psi} - M_{\eta_c}$, for example; some even awaits further more accurate experiments: the charmonium radiative transition rate $\Gamma_{J/\psi \rightarrow \gamma \eta_c}$ and the decay constant f_{D_s} . There are also quantities that the lattice cannot compute accurately enough. An example is the muon $g - 2$, a quantity showing 3.6σ deviation from the standard model. It is feasible to compute the leading hadronic contributions from

QCD first principles, however, more efforts are needed to bring down the error bars in future lattice calculations. It is in this constant process of comparison between the experiments and theory that we could sharpen our understanding of the theory of strong interaction.

Acknowledgments

This work is supported in part by the National Science Foundation of China (NSFC) under the project No. 11335001 and No.11021092. It is also supported in part by the DFG and the NSFC (No.11261130311) through funds provided to the Sino-German CRC 110 “Symmetries and the Emergence of Structure in QCD”.

References

1. *Lattice 2013 Homepage*. http://www.lattice2013.uni-mainz.de/37_ENG_HTML.php.
2. *Lattice 2013 webpage*. <http://www.lattice2013.uni-mainz.de/presentations/Plenaries%20Saturday/Thomas.pdf>.
3. M. Lüscher and U. Wolff, *Nucl.Phys.* **B339**, 222 (1990).
4. J. J. Dudek, R. G. Edwards, M. J. Peardon, D. G. Richards and C. E. Thomas, *Phys.Rev.* **D82**, p. 034508 (2010).
5. S. Durr, Z. Fodor, J. Frison, C. Hoelbling, R. Hoffmann *et al.*, *Science* **322**, 1224 (2008).
6. C. McNeile, C. Davies, E. Follana, K. Hornbostel and G. Lepage, *Phys.Rev.* **D86**, p. 074503 (2012).
7. M. Lüscher, *Nucl.Phys.* **B354**, 531 (1991).
8. *Lattice 2013 webpage*. <http://www.lattice2013.uni-mainz.de/presentations/Plenaries%20Saturday/Doring.pdf>.
9. J. J. Dudek, R. G. Edwards and C. E. Thomas, *Phys.Rev.* **D87**, p. 034505 (2013).
10. N. Li and C. Liu, *Phys.Rev.* **D87**, p. 014502 (2013).
11. S. Choi *et al.*, *Phys.Rev.Lett.* **91**, p. 262001 (2003).
12. B. Aubert *et al.*, *Phys.Rev.Lett.* **95**, p. 142001 (2005).
13. S. Choi *et al.*, *Phys.Rev.Lett.* **100**, p. 142001 (2008).
14. M. Ablikim *et al.*, *Phys.Rev.Lett.* **110**, p. 252001 (2013).
15. G.-Z. Meng *et al.*, *Phys.Rev.* **D80**, p. 034503 (2009).
16. S. Prelovsek and L. Leskovec, *arXiv:1307.5172* (2013).
17. S. Prelovsek and L. Leskovec, *arXiv:1308.2097* (2013).
18. A. S. Kronfeld, *arXiv:0912.0543* (2009).
19. E. Follana, C. Davies, G. Lepage and J. Shigemitsu, *Phys.Rev.Lett.* **100**, p. 062002 (2008).
20. *Heavy Flavor Averaging Group*, (2010). <http://www.slac.stanford.edu/xorg/hfag/charm/index.html>.
21. C. Davies, C. McNeile, E. Follana, G. Lepage, H. Na *et al.*, *Phys.Rev.* **D82**, p. 114504 (2010).
22. *Lattice 2013 webpage*. <http://www.lattice2013.uni-mainz.de/presentations/6C/Bernard.pdf>.
23. J. J. Dudek, R. G. Edwards and D. G. Richards, *Phys.Rev.* **D73**, p. 074507 (2006).
24. Y. Chen, D.-C. Du, B.-Z. Guo, N. Li, C. Liu *et al.*, *Phys.Rev.* **D84**, p. 034503 (2011).
25. G. Donald, C. Davies, R. Dowdall, E. Follana, K. Hornbostel *et al.*, *Phys.Rev.* **D86**, p. 094501 (2012).

12 *C. Liu*

26. D. Becirevic and F. Sanfilippo, *JHEP* **1301**, p. 028 (2013).
27. R. Mitchell *et al.*, *Phys.Rev.Lett.* **102**, p. 011801 (2009).
28. L.-C. Gui, Y. Chen, G. Li, C. Liu, Y.-B. Liu *et al.*, *Phys.Rev.Lett.* **110**, p. 021601 (2013).
29. Y.-B. Yang, L.-C. Gui, Y. Chen, C. Liu, Y.-B. Liu *et al.*, *Phys.Rev.Lett.* **111**, p. 091601 (2013).
30. Y.-B. Yang, Y. Chen, L.-C. Gui, C. Liu, Y.-B. Liu *et al.*, *Phys.Rev.* **D87**, p. 014501 (2013).
31. J. Beringer *et al.*, *Phys.Rev.* **D86**, p. 010001 (2012).
32. T. Blum, *Phys.Rev.Lett.* **91**, p. 052001 (2003).
33. M. Gockeler *et al.*, *Nucl.Phys.* **B688**, 135 (2004).
34. C. Aubin and T. Blum, *Phys.Rev.* **D75**, p. 114502 (2007).
35. X. Feng, K. Jansen, M. Petschlies and D. B. Renner, *Phys.Rev.Lett.* **107**, p. 081802 (2011).
36. P. Boyle, L. Del Debbio, E. Kerrane and J. Zanotti, *Phys.Rev.* **D85**, p. 074504 (2012).
37. M. Della Morte, B. Jager, A. Juttner and H. Wittig, *JHEP* **1203**, p. 055 (2012).
38. *Lattice 2013 webpage*. <http://www.lattice2013.uni-mainz.de/static/HStr.html#contrib4120>.
39. *Lattice 2013 webpage*. <http://www.lattice2013.uni-mainz.de/presentations/9B/Gregory.pdf>.
40. F. Burger, X. Feng, G. Hotzel, K. Jansen, M. Petschlies *et al.*, *arXiv:1308.4327* (2013).